AMERICAN SOCIETY FOR MICROBIOLOGY | Antimicrobial Agents and Chemotherapy®

PHARMACOLOGY

Plasma and Cerebrospinal Fluid Population Pharmacokinetics of Vancomycin in Patients with External Ventricular Drain

Zhendong Chen,[a] Max Taubert,[a] Chunli Chen,[a,b] Charalambos Dokos,[a] Uwe Fuhr,[a] Thomas Weig,[c] Michael Zoller,[c] Suzette Heck,[d] Konstantinos Dimitriadis,[d,e] Nicole Terpolilli,[e,f] Christina Kinast,[c] Christina Scharf,[c] Constantin Lier,[g] Christoph Dorn,[g] Uwe Liebchen[c]

[a]Department I of Pharmacology, Center for Pharmacology, Faculty of Medicine and University Hospital Cologne, University of Cologne, Cologne, Germany
[b]Heilongjiang Key Laboratory for Animal Disease Control and Pharmaceutical Development, College of Veterinary Medicine, Northeast Agricultural University, Harbin, People's Republic of China
[c]Department of Anesthesiology, University Hospital, Ludwig Maximilians University of Munich, Munich, Germany
[d]Department of Neurology, University Hospital, Ludwig Maximilian University, Munich, Germany
[e]Institute for Stroke and Dementia Research (ISD), University Hospital, Ludwig Maximilians University, Munich, Germany
[f]Department of Neurosurgery, Munich University Hospital, Munich, Germany
[g]Institute of Pharmacy, Faculty of Chemistry and Pharmacy, University of Regensburg, Regensburg, Germany

ABSTRACT Vancomycin is a commonly used antibacterial agent in patients with primary central nervous system (CNS) infection. This study aims to examine predictors of vancomycin penetration into cerebrospinal fluid (CSF) in patients with external ventricular drainage and the feasibility of CSF sampling from the distal drainage port for therapeutic drug monitoring. Fourteen adult patients (9 with primary CNS infection) were treated with vancomycin intravenously. The vancomycin concentrations in blood and CSF (from proximal [CSF_P] and distal [CSF_D] drainage ports) were evaluated by population pharmacokinetics. Model-based simulations were conducted to compare various infusion modes. A three-compartment model with first-order elimination best described the vancomycin data. Estimated parameters included clearance (CL, 4.53 L/h), central compartment volume (V_c, 24.0 L), apparent CSF compartment volume (V_{CSF}, 0.445 L), and clearance between central and CSF compartments (Q_{CSF}, 0.00322 L/h and 0.00135 L/h for patients with and without primary CNS infection, respectively). Creatinine clearance was a significant covariate on vancomycin CL. CSF protein was the primary covariate to explain the variability of Q_{CSF}. There was no detectable difference between the data for sampling from the proximal and the distal port. Intermittent infusion and continuous infusion with a loading dose reached the CSF target concentration faster than continuous infusion only. All infusion schedules reached similar CSF trough concentrations. Beyond adjusting doses according to renal function, starting treatment with a loading dose in patients with primary CSF infection is recommended. Occasionally, very high and possibly toxic doses would be required to achieve adequate CSF concentrations, which calls for more investigation of direct intraventricular administration of vancomycin. (This study has been registered at ClinicalTrials.gov under registration no. NCT04426383).

KEYWORDS vancomycin, population pharmacokinetics model, distal port, CSF protein, central nervous system infection, ventriculitis

External ventricular drainage (EVD) is a common procedure in neurocritical care units to monitor and treat intracranial pressure by draining cerebrospinal fluid (CSF) (1). However, an EVD-associated infection is a serious nosocomial complication and is associated with significant morbidity and mortality in neurocritical patients (1). Insufficient penetration of antimicrobials into the CSF after intravenous administration could contribute to therapeutic failure (2). This often results in the selection of high doses, which in turn

Address correspondence to Zhendong Chen, zhendong.chen@uk-koeln.de.

The authors declare no conflict of interest.

Received 22 February 2023
Returned for modification 21 March 2023
Accepted 15 April 2023
Published 10 May 2023

increases the risk for systemic adverse effects. It is therefore particularly important in patients suffering from EVD-related infections to individualize the dose of antibiotics to achieve a timely effective concentration in the CSF.

Due to the occurrence of Gram-positive penicillin-resistant pathogens, vancomycin is a standard therapy for central nervous system (CNS) infections, specifically, nosocomial infections (3). Nowadays, the plasma pharmacokinetics (PK) of vancomycin have been well investigated by many studies (4–9), and various population pharmacokinetics (PopPK) models based on plasma concentrations have also been reported for different populations, including adults, critically ill patients, pediatric patients, neonate patients, etc. (10). In most of these models, total body weight (TBW) and/or creatinine clearance (CrCL) were confirmed as significant covariates on vancomycin clearance, since vancomycin is primarily eliminated by the kidney in unchanged form (10). Therefore, predictable vancomycin plasma concentrations can be obtained using these models (11).

However, vancomycin cannot easily penetrate the blood-brain barrier (BBB) into the CSF due to its pronounced hydrophilicity and high molecular weight (12). Vancomycin CSF concentrations are highly variable and unpredictable in most cases, because the extent of vancomycin penetration depends greatly on the integrity of the BBB (13–15). BBB damage caused by inflamed meninges has also been proven to enhance the penetration of vancomycin into the CSF. So far, only a few studies have investigated the pharmacokinetics of vancomycin, reporting several validated PopPK models in which CSF albumin or lactate concentrations were related to the distribution of vancomycin into the CSF, thus helping to predict CSF concentrations after intravenous administration (16–18). The available data in individual studies are sparse, the validation of developed predictors is limited, and there is still insufficient knowledge about vancomycin CSF penetration and the respective covariates in neurological/neurosurgical patients. Therefore, the main aim of this study was to investigate predictors for vancomycin penetration into CSF. To this end, a new PopPK model was developed and validated based on vancomycin plasma and CSF data from patients who had an EVD. The feasibility of collecting CSF samples at the distal port of the EVD system for therapeutic drug monitoring (TDM) was assessed using this new PopPK model. Finally, the benefits of different infusion modes and dosages were examined through model-based simulations.

RESULTS

Patient characteristics. A total of 190 plasma samples and 232 CSF samples, including 22 samples taken from the proximal port (CSF_P) and 210 samples taken from the distal port (CSF_D), were collected from 14 patients with EVDs in this study (for an illustration of the drainage system, see reference 19). Among the 14 patients, 9 with CNS infection and 5 without primary CNS infection, 11 were men and 3 were women, with a mean age of 52 years (range, 22 to 77 years). The main patient characteristics are shown in Table 1. Detailed information on disease for each patient, as well as the vancomycin infusion mode and additional covariate values, including the values for unbound fraction (f_u), albumin, bilirubin, C-reactive protein, leukocytes, and interleukin 6 and ferritin (CSF), erythrocytes (CSF), cell count (CSF), and interleukin 6 (CSF), are shown in Tables S1 and S2 in the supplemental material.

Population pharmacokinetics model. A two-compartment model with first-order elimination and proportional residual error best described the vancomycin plasma data. The base plasma model was parameterized by vancomycin clearance (CL), central compartment volume (V_c), intercompartment clearance (Q_p), and peripheral compartment volume (V_p). Before the inclusion of any covariates, the interindividual variables (IIVs) of CL, Q_p, and V_p were estimated to be 38.5%, 93.7%, and 53.8%, respectively. Significant effects of CrCL on CL (change in objective function value [ΔOFV] = −4.073) and of age on Q_p (ΔOFV = −10.585) were found, resulting in reductions of IIVs to 30.8% and 35.1% for CL and Q_p, respectively. Other clinical characteristics, including sex, weight, height, body surface area (BSA), estimated glomerular filtration rate (eGFR), and f_u, were eliminated due to showing no significant contribution to ΔOFV.

On the basis of the final plasma model, two different CSF models, including the transit compartment model and the bulk flow model, were compared to fit the vancomycin CSF

TABLE 1 Demographics and covariates of subjects

Characteristic[a]	No. or mean value (SD) for patients:	
	With primary CNS infection	Without primary CNS infection
Demographics		
Male	7	4
Female	2	1
Age (yr)	59.7 (11.8)	37.0 (10.2)
Body wt (kg)	84.2 (25.0)	88.6 (16.6)
Ht (cm)	174 (6)	179 (9)
Covariates		
In plasma		
Creatinine (mg/dL)	0.671 (0.138)	0.693 (0.287)
CrCL (mL/min)	142 (57)	194 (41)
In CSF		
Protein (mg/dL)	108 (53)	27.4 (29.0)
S100 protein (μg/L)	3.88 (2.13)	30.0 (0.0)
Glucose (mg/dL)	51.4 (21.7)	80.4 (13.5)
NSE (μg/L)	15.6 (4.9)	326 (199)
Lactate (mmol/L)	4.63 (0.98)	1.78 (0.43)

[a]CrCL, creatinine clearance estimated by the Cockcroft-Gault equation; NSE, neuron-specific enolase concentration. For further parameters, see Table S2.

data separately. Little difference was found in either goodness-of-fit (GOF) plots or change in Akaike information criterion (ΔAIC) (1.711) between two different CSF models, which were subsequently analyzed for CSF-related covariates in parallel. However, the bulk flow model showed better correlations between Q_{CSF} and all covariates than the transit compartment model, and it had a lower AIC when including a particular Q_{CSF}-related covariate. Therefore, the bulk flow model was ultimately chosen for the base CSF model.

Five CSF-related covariates, including CSF protein, S100 protein, glucose, neuron-specific enolase (NSE), and lactate concentrations in CSF, were found to have significant effects on Q_{CSF} separately, and the ΔOFVs were −29.755, −9.868, −9.394, −7.582, and −6.587, respectively. The regression plots of the Q_{CSF} versus the concentrations of each CSF-related covariate are shown in Fig. S1. Due to the multicollinearity and reasonable physiological considerations, only the CSF protein concentration was included in the final CSF model, which led to a decrease from 165.6% to 36.6% in the IIV of Q_{CSF}. Primary CNS infection was found to be a significant covariate both for Q_{CSF} and the protein covariate effect, resulting in decreases in the OFVs of 5.152 and 6.959, respectively. Therefore, two separate equations were generated to estimate the vancomycin penetration in patients with and without primary CNS infection. The relationships between random effects (η) and the significant covariates in the base model and the final model are shown in Fig. S2.

All parameter estimates remained essentially unchanged after the exclusion of CSF_P data (not shown). The proportional residual errors for CSF_P and CSF_D samples were estimated to be 25.2% and 27.8%, respectively, and the separation of the error models for each of them did not improve the CSF model fitting (ΔOFV = −0.256). This indicated little difference in the accuracy of vancomycin concentrations between the two types of CSF samples. Therefore, only one proportional residual error model was used for both the CSF_P and CSF_D samples in the final CSF model. The final model equations for CL, Q_p, and Q_{CSF} are presented below:

$$\mathrm{CL} = \left(\frac{\mathrm{CrCL}}{170}\right)^{0.461} \times \mathrm{TVCL} \times e^{\eta_1}$$

$$Q_p = \left(\frac{\mathrm{age}}{48}\right)^{2.61} \times \mathrm{TVQ}_p \times e^{\eta_2}$$

For patients with primary CNS infection,

TABLE 2 Parameter estimates and bootstrap results from the final model

	Value(s) for:			
	Final model		927 successful bootstrap runs (n = 1,000)	
Parameter[a]	Estimate	RSE (%)[b]	Median	95% CI[c]
CL (L/h)	4.53	7.5	4.52	3.74–5.29
V_c (L)	24.0	8.6	23.3	16.6–27.0
Q_p (L/h)	5.69	12.2	5.70	4.43–8.64
V_p (L)	38.7	16.5	39.7	27.9–59.1
Q_{CSF}_1 (L/h)	0.00322	5.6	0.00331	0.00263–0.00390
Q_{CSF}_2 (L/h)	0.00135	29.9	0.00129	0.000938–0.00383
V_{CSF} (L)	0.445	14.7	0.465	0.244–0.883
Covariates				
CrCL on CL	0.453	27.6	0.452	0.150–0.830
Age on Q_p	2.69	24.4	2.84	1.37–4.74
Protein (CSF) on Q_{CSF}_1	1.09	6.0	1.10	0.808–1.67
Protein (CSF) on Q_{CSF}_2	0.575	21.9	0.575	0.203–1.03
Interindividual variability (%)				
CL	29.5 (0.1)[d]	18.7	27.9	15.9–38.1
V_p	54.3 (20.6)	25.1	54.9	21.4–93.7
Q_{CSF}	19.8 (17.7)	20.8	13.6	4.7–25.1
V_{CSF}	94.2 (10.1)	20.8	105.0	36.1–175.7
Residual variability (proportional error) (%)[e]				
Plasma	15.9 (5.3)[d]	15.5	15.4	10.7–20.4
CSF	27.5 (3.8)	5.6	26.5	17.3–34.7

[a]CL, clearance; V_c, central compartment volume; Q_p, intercompartment clearance between central and peripheral compartments; V_p, peripheral compartment volume; Q_{CSF}_1, intercompartment clearance between plasma and CSF compartment in patients with primary CNS infection; Q_{CSF}_2, intercompartment clearance between plasma and CSF compartment in patients without primary CNS infection; V_{CSF}, CSF compartment volume; CrCL, creatinine clearance.
[b]RSE, relative standard error.
[c]CI, confidence interval.
[d]Shrinkage estimates of interindividual variability (IIV) and residual variability are shown in parentheses.
[e]Proportional residual error is expressed as the coefficient of variation (CV).

$$Q_{CSF} = \left(\frac{\text{CSF protein}}{84}\right)^{1.09} \times \text{TVQ}_{CSF}\_1 \times e^{\eta_3}$$

For patients without primary CNS infection,

$$Q_{CSF} = \left(\frac{\text{CSF protein}}{84}\right)^{0.575} \times \text{TVQ}_{CSF}\_2 \times e^{\eta_3}$$

where TVCL, TVQ_p, TVQ_{CSF}_1, and TVQ_{CSF}_2 are the typical population values for CL, Q_p, Q_{CSF}_1, and Q_{CSF}_2, respectively.

The final model parameter estimates and the 95% confidence intervals for the results of 1,000 bootstrap analyses are displayed in Table 2. As shown, all relative standard errors (RSEs) for PK parameters were less than 30%, which demonstrated acceptable precision. The IIV shrinkages of CL, V_p, Q_{CSF}, and V_{CSF} both in the base model and the final model (Table 2) were all below 30%, which was considered acceptable. The consistency between original parameter estimates and median values estimated from the bootstrap analysis proved the model was stable. The GOF plots for model diagnosis are displayed in Fig. 1. The inclusion of covariates significantly improved the model diagnostic plots. A satisfactory fit was subsequently obtained between observed and predicted values, with no trends of conditional weighted residuals over time for either plasma or CSF samples. Figure 2 shows the prediction-corrected visual predictive checks (pcVPCs) of the final model, which indicated that the model captured the central tendency and distribution of most observed data points both in plasma and CSF. However, the 95% percentile observed in the CSF lies at the inner boundary of the

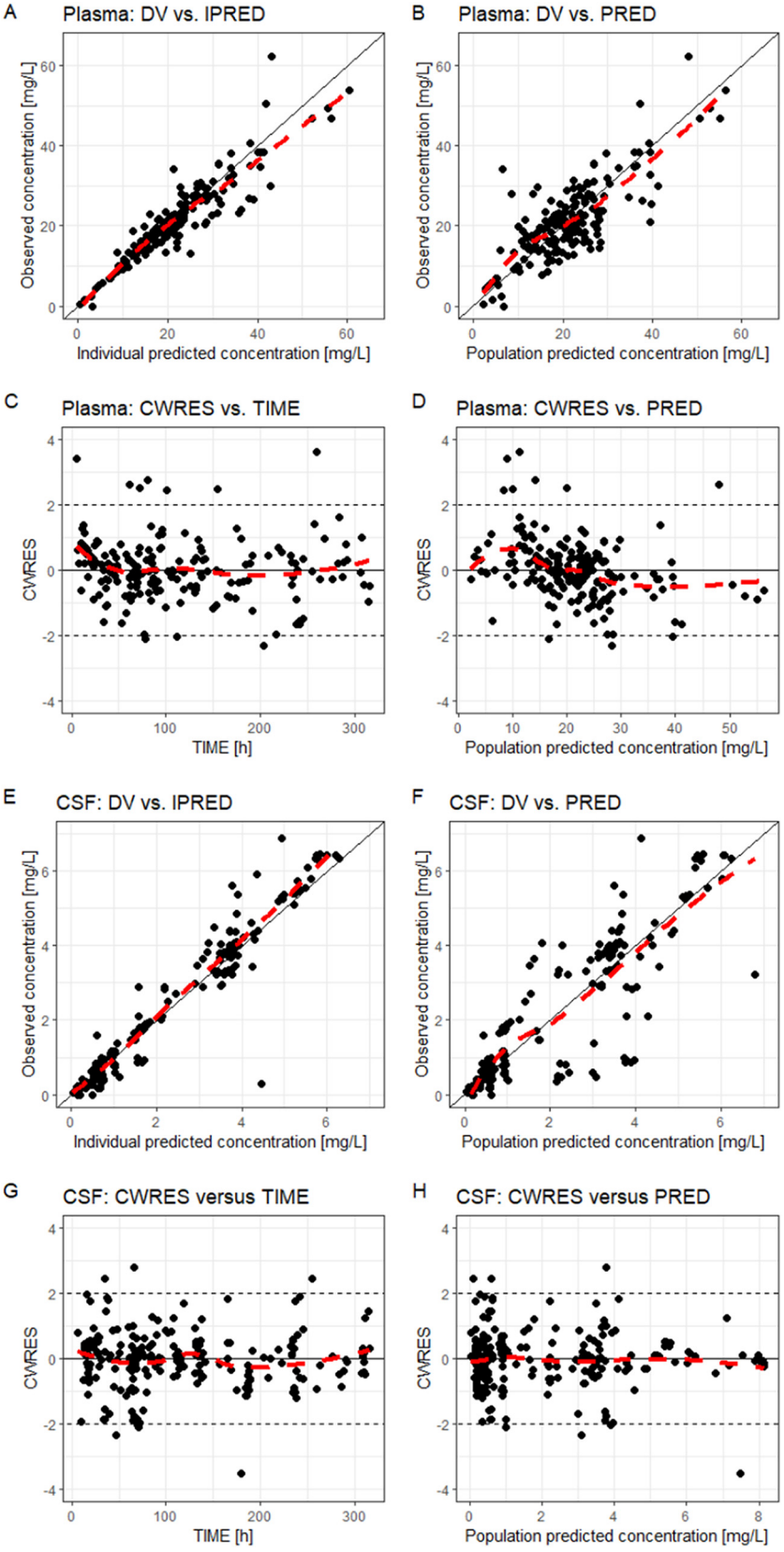

FIG 1 Combined goodness-of-fit plots of the final model for vancomycin plasma (A to D) and CSF (E to H) concentrations. DV, observed concentrations; IPRED, individual predicted concentrations; PRED, population predicted concentrations; CWRES, conditional weighted residuals; TIME, time after the first dose. Red lines show the local polynomial regression fit.

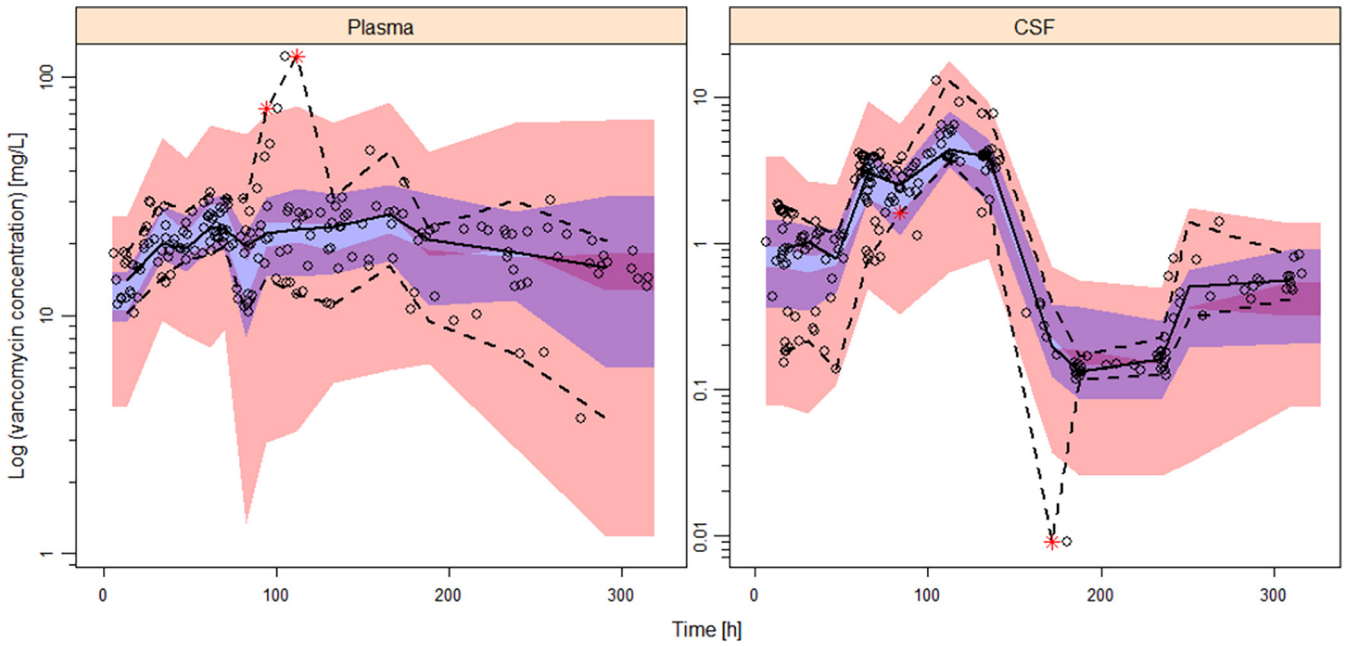

FIG 2 Confidence interval prediction-corrected visual predictive check (n = 1,000) for the final model for plasma and CSF. Dots represent observed concentrations. Black solid lines represent the median values, while dashed lines show the 5th and 95th percentiles of observed concentrations. Shaded areas are the model-predicted 95% confidence intervals for the 5th (red), 50th (blue), and 95th (red) percentiles from 1,000 simulated data sets.

respective confidence intervals, which may be due to the large variability of the V_{CSF}. Individual plots of observed concentrations and concentrations predicted by the final model in plasma and CSF are displayed in Fig. S3 and S4, respectively.

Comparisons of parameter estimates and calculations of probability of target attainment (PTA) for the sensitivity analysis with individual adjustment of CSF_D sampling times are shown in Tables S3 and S4. The parameter estimates remained nearly unchanged except for V_{CSF}, which had a lower estimate when using earlier sampling times for CSF_D samples. The PTA ratios for both plasma and CSF targets between the two models ranged from 0.83 to 1.29, indicating no relevant difference. When assuming a uniform CSF flow rate of 12 or 36 mL/min (20), the respective adjustments in sampling times had essentially no effect on any parameter estimates or on PTA calculations (data not shown). Therefore, the uncertainty of the CSF flow rate and the related time delay for CSF_D samples is irrelevant for the model's application, and assuming no delay between CSF_P and CSF_D samples in this study is justifiable.

Simulations. Changes in the vancomycin plasma area under the concentration-time curve over 24 h (AUC_{24}) and CSF trough concentration (C_{trough}) in patients with different CrCL values and concentrations of CSF protein under different dosing regimens are shown in Fig. S5 and S6, respectively. The simulation results suggested that CrCL showed a moderate effect on CL but CSF protein had a large effect on Q_{CSF}. The multitude of covariates did not allow standard dosing recommendations in this study.

The probabilities of target attainment (PTA) in simulated patients with primary CNS infection after different dosing regimens of vancomycin are listed in Table 3. On the first day of vancomycin treatment, there were only minor differences in plasma AUC_{24} values between intermittent infusion and continuous infusion with a loading dose, but there were relatively lower plasma AUC_{24} values for continuous infusion without a loading dose. A daily dose of 2 g vancomycin was sufficient to achieve the target plasma ratio of AUC_{24} to MIC (AUC_{24}/MIC = 400) at MICs of $\leq$0.5 mg/L in $>$90% of simulated patients, regardless of the renal function, whether administration was by intermittent infusion or continuous infusion with a loading dose. If the MIC was 1 mg/L, a daily dose of 3 g was sufficient for 84.4% of simulated patients with CrCL of $<$150 mL/min, whereas patients with CrCL of $>$150 mL/min might require a daily dose of 4 g, which was the recommended

TABLE 3 Probability of target attainment in simulated patients with primary central nervous system infection after different dosing regimens of vancomycin

	Values [day 1 (steady state)] for indicated type and amt (g) of dose/24 h[b]								
	II (q12h)			CI_L			CI		
PK/PD target[a]	2	3	4	2	3	4	2	3	4
Plasma AUC_{24} (mg · h/L)									
>200	96.0 (98.8)	99.9 (99.9)	100 (100)	94.5 (98.7)	99.9 (100)	100 (100)	84.1 (99.0)	99.7 (100)	100 (100)
>400	12.0 (56.9)	72.4 (91.3)	96.0 (98.8)	11.3 (59.6)	67.1 (92.1)	94.5 (98.7)	0.7 (61.7)	36.1 (92.7)	84.1 (99.0)
>600	0.1 (15.5)	12.0 (56.9)	54.0 (85.6)	0 (17.0)	11.3 (59.6)	48.2 (85.8)	0 (17.7)	0.7 (61.7)	17.3 (87.3)
CSF C_{trough} (mg/L)									
>0.5	87.5 (98.4)	94.0 (99.7)	96.7 (100)	87.1 (99.0)	94.1 (99.9)	96.8 (100)	86.4 (99.3)	93.4 (99.9)	96.6 (100)
>1.0	64.2 (89.2)	80.7 (96.0)	87.5 (98.4)	62.5 (92.0)	78.7 (97.4)	87.1 (99.1)	64.3 (92.4)	78.7 (97.8)	86.4 (99.3)
>2.0	27.6 (63.7)	49.9 (81.4)	64.2 (89.2)	23.5 (70.3)	47.6 (85.7)	62.5 (92.0)	29.7 (70.1)	51.0 (85.8)	64.3 (92.4)

[a]AUC_{24}, daily area under the curve; C_{trough}, the concentration at 24 h or 120 h after the first dose for day 1 or steady state, respectively.
[b]II, intermittent infusion; CI_L, continuous infusion with a loading dose same as the first does of II; CI, continuous infusion without a loading dose.

daily dose for continuous infusion by Jalusic et al. (18) For different known pathogens, the daily dose could be optimized to adapt the respective target AUC_{24}/MIC for all populations.

Simulated time-concentration profiles in plasma and CSF after different dosing regimens over 5 days are displayed in Fig. 3. The three infusion modes with the same daily dose resulted in similar levels of C_{trough} in CSF on day 1 and at steady state, but intermittent infusion and continuous infusion with a loading dose allowed the presumed same target concentrations in CSF to be reached faster than continuous infusion without a loading dose did. In contrast, continuous infusion could keep plasma concentrations relatively low during the therapy. Therefore, continuous infusion, especially at high doses, is recommended to avoid higher vancomycin plasma concentrations, which may help reduce renal toxicity (21). If the target C_{trough} in CSF was 1 mg/L, adjustment of doses according to CSF protein concentrations of ≥150, <150 and ≥100, and <100 mg/dL resulted in daily doses of 2, 3, and 4 g vancomycin, which were then linked to PTAs of 90.4%, 90.8%, and 69.6%, respectively, in simulated patients. As a concern for patients with primary CNS infection, a daily dose of 4 g vancomycin would cause at least 17.3% of patients to face a potential plasma AUC_{24} above 600 mg · h/L, which may lead to a higher risk of acute kidney injury (AKI) (22). Excessive systemic exposure would also prohibit using even higher vancomycin doses in order to achieve higher CSF PTAs in patients with low CSF protein concentrations.

DISCUSSION

In the present study, a PopPK model of vancomycin was successfully developed based on 14 patients with EVDs to examine potential surrogate parameters for the vancomycin penetration rate from plasma to CSF. The time courses of the plasma and CSF concentrations of vancomycin were best described by a linear three-compartment model (contains a CSF compartment). The difference in residual unexplained variability of CSF samples collected at the proximal and the distal port of the EVD system as assessed by residual error models showed that sampling at the distal port is feasible. The probability of PK/pharmacodynamics (PD) target attainment by AUC_{24}/MIC or MIC was subsequently evaluated across different dosing regimens with Monte Carlo simulations.

The plasma PK of vancomycin in different populations have been well investigated by a number of studies. Compared with the published models, the parameter estimate for CL (4.54 L/h) in our model was consistent with reported values, and in accordance with previous studies, CrCL showed a significant effect on CL (16–18, 23, 24). In addition, an additional finding of this study was that age was well correlated with Q_p, suggesting faster distribution of vancomycin into tissues with increasing age. The difference from the published models lies in the V_p, which was estimated at 38.6 L in this study, and no significant covariate on V_p was found. In similar studies about PopPK models in patients who underwent EVD, Li reported a value of 19.8 L for V_p and Jalusic fixed the value at

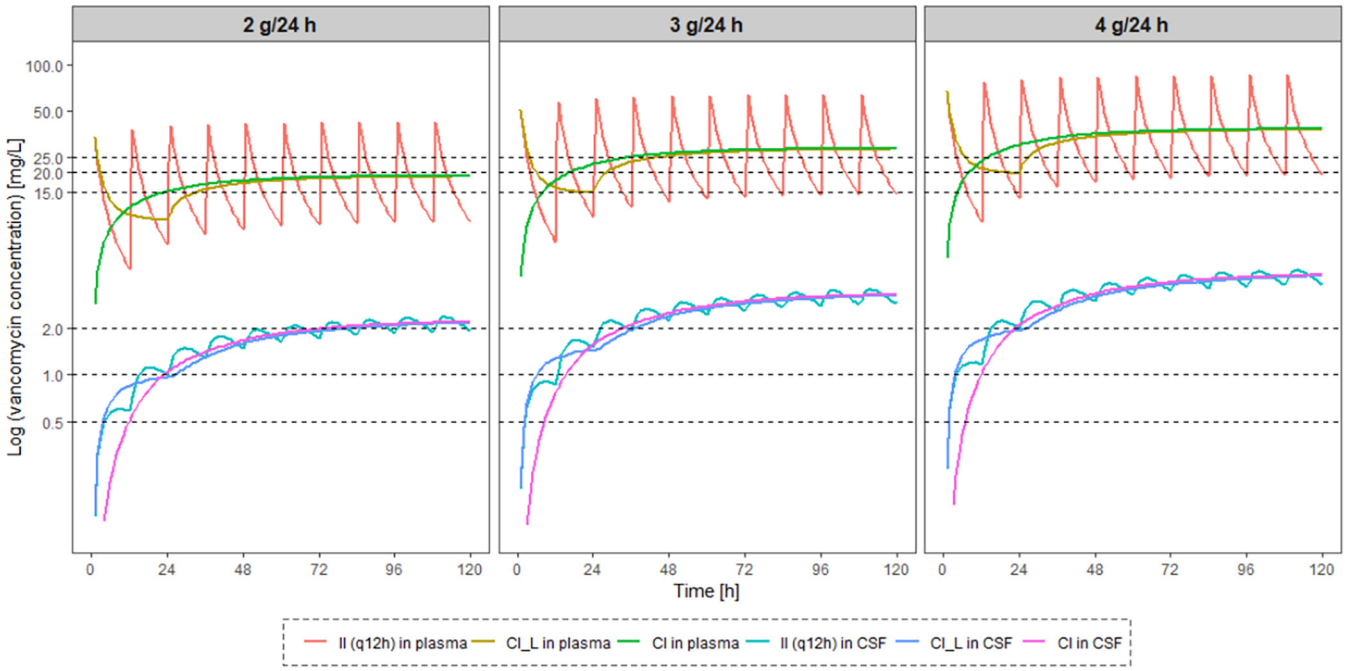

FIG 3 Median concentration-versus-time curves simulated in plasma and CSF after different dosing regimens of vancomycin over 5 days in patients with CNS infection. II, intermittent infusion; q12h, every 12 h; CI_L, continuous infusion with a loading dose same as the first dose of q12h; CI, continuous infusion without a loading dose.

86.2 L in their final model (17, 18). This discrepancy might be due to the different distributions of sampling points in different studies (17). Compared with Jalusic's model, more time points close to the peak were used to build the model in this study, and thus, the estimation of V_p may be closer to the true value.

In addition to the reported CSF lactate concentration, four additional potential surrogate parameters, CSF protein, S100 protein, glucose, and NSE, were identified as showing good correlations with vancomycin penetration from plasma to CSF using the bulk flow model. In accordance with the previous finding, the elevation of CSF protein and lactate concentrations, as well as the reduction of CSF glucose concentration, can suggest CNS infection with BBB damage, which could lead to easier penetration of vancomycin into CSF (18, 25, 26). However, the correlations of increased CSF S100 protein and NSE concentrations to decreased Q_{CSF} are not in agreement with other findings, where higher CSF S100 protein and NSE concentrations were found in patients with CNS infection (27, 28). This discrepancy may be due to the small sample size of this study or limitations of the structural CSF model.

Typically, it is common to collect CSF samples at the proximal port of the EVD system, which is closest to the head. In contrast, collecting CSF samples via a distal overflow system is easier and safer for minimizing the infection risk (19, 29) but will cause a time delay in drug concentrations for TDM. No delay between CSF_P and CSF_D samples was assumed in the present study because the spaces were not fully separated and diffusion might play a role in the propagation of vancomycin concentrations, in addition to flow rate. Moreover, the concentration measured in a CSF_D sample represents an average concentration over a period instead of the concentration at a certain time. Kinast et al. and Wong confirmed no significant differences in the concentrations of substances, including total protein, glucose, and lactate, between the CSF samples from the two sites (19, 29). To our knowledge, no such studies so far have investigated the feasibility of using CSF_D samples for TDM of vancomycin or other drugs. In this study, the residual errors of CSF_P and CSF_D samples were compared using separate proportional residual error models, and no statistically significant difference was found. In addition, the sensitivity analyses assuming various degrees of delay for CSF_D samples showed no meaningful

impact of the CSF sampling site. Therefore, collecting CSF samples at the distal port of the EVD system for TDM or Bayesian dosing approaches of vancomycin could be a valuable choice in the future. It is worth noting that careful documentation of the start and end times of collecting CSF_D samples is critical to calculating the applicable time, thus reducing potential error (30).

A previous PK/PD target tentatively suggested for vancomycin TDM was a plasma C_{trough} of 15 to 20 mg/L for adult patients, but data supporting this target are very limited (31). Recent evidence shows that a more reliable PK/PD target in plasma is an AUC_{24}/MIC of $\geq$400, taking into account efficacy and safety (22), as the AKI risk was significantly less with AUC-guided monitoring than with C_{trough}-guided monitoring (32). Furthermore, there are also studies evaluating the relationship between the daily vancomycin AUC and AKI, and these suggested that the AUC_{24} in plasma should be maintained between 400 and 600 mg · h/L to maximize efficacy and minimize toxicity (22). However, an AUC_{24}/MIC of $\geq$400 in CSF is hardly achievable, due to the limited vancomycin penetration from plasma to CSF. Monitoring the AUC in CSF by a rich sampling strategy during TDM is also cumbersome in practice for intermittent infusions, and an AUC_{24} of $\geq$400 is not achievable in most cases (33). At the same time, no such relevant PK/PD target in CSF was defined so far for optimizing dosing regimens for patients with CNS infection (34). Therefore, simulations in this study were performed using both the AUC_{24} in plasma and the C_{trough} in CSF as PK/PD targets to obtain PTA in different dosing regimens. Because there was no significant difference in vancomycin CL between patients with and without primary CNS infection, subsequent simulations were only conducted in patients with primary CNS infection. The reported protein binding (PB) of vancomycin in plasma is approximately 50% (3), while the mean PB of the 14 subjects in the present study was 70.1% (63.9 to 82.7%) and was highly variable. The inclusion of individual f_u as a covariate for the CSF volume of distribution or Q_{CSF} did not help to improve the model fit and was therefore not considered. The PB of vancomycin in CSF was also not taken into account, because the highest CSF protein concentration (2.26 mg/mL) reported in the present study is still far from the normal protein concentration in plasma (60 to 70 mg/mL) (35), suggesting that the total CSF concentrations of vancomycin are essentially equal to the unbound concentrations.

Based on our simulation results, a starting daily dose of 2, 3, or 4 g was recommended for patients with a CSF protein concentration of $\geq$150, $<$150 and $\geq$100, or $<$100 mg/dL, respectively. In the meantime, continuous infusion with a loading dose of vancomycin is recommended for patients with CNS infection. On the first day of the treatment, intermittent infusion could lead to a steep increase in the vancomycin concentration in CSF, which is helpful to achieve a target concentration in CSF faster than by continuous infusion. Afterwards, continuous infusion could be used to maintain an adequate plasma concentration, to avoid potential AKI and nephrotoxicity (21, 34). In addition, a dose of vancomycin such as 4 g/24 h was recommended for achieving an adequate CSF vancomycin concentration in other studies, but this dose resulted in a plasma AUC_{24} exceeding 600 mg · h/L on day 1 and at steady state in at least 17.3% and 85.6% of simulated patients, respectively. Therefore, it is recommended that dose adjustment should be made in a timely manner after adequate CSF concentrations have been obtained, based on TDM results and Bayesian predictions via the PopPK method. The proposed final model in this study could be employed after external evaluation and software integration.

For the treatment of patients with CNS infection, combined intravenous (i.v.) and intraventricular (i.v.t.) administration of vancomycin is becoming increasingly popular for first applications (22). The doses for i.v.t. reported in the literature ranged from 0.075 to 50 mg/day, and the CSF vancomycin concentrations varied widely, from 1.1 to 812.6 mg/L (36). Tentatively, simulations using the same dosages as reported in the literature were performed using our model established herein. The results showed that the predicted plasma concentrations for combined administration at most time points were close to the reported values, but the predicted CSF concentrations at all points in time were less than the reported values. This underestimation may be caused by the predicted (empirical) V_{CSF}

(0.445 L) in this study being larger than the actual human V_{CSF} (approximately 0.15 L). Obstruction of CSF circulation due to hydrocephalus or surgery may also result in CSF concentrations in actual CSF samples being higher than expected if vancomycin was evenly distributed in the CSF (36, 37). Therefore, our model using only data after intravenous administration was unable to predict CSF concentrations after combined i.v. and i.v.t. administration (36, 38). Despite the apparent underprediction of CSF concentrations compared to those obtained with real combined i.v./i.v.t. administration, our predicted CSF C_{trough} would exceed 10 mg/L in most patients after 20 mg i.v.t. with 2 g i.v. every 24 h, while the predicted plasma AUC would remain at a safe and effective level. This indicates that the combined administration could be a better choice to improve the outcome of patients with CNS infection in the future and should be further investigated.

Several limitations remain in this study. Only 14 patients were included and not all covariates were available for all patients, and thus, correlations between different CSF-related covariates and Q_{CSF} could not be compared. In addition, the small sample size precluded the use of a more stringent backward-elimination strategy for the covariance model. The final model still retains unexplained IIVs of 19.8% and 94.2% for Q_{CSF} and V_{CSF}, respectively. Relatively limited data for CSF_P samples were supported to compare the residual error of CSF_P and CSF_D samples. No vancomycin data for i.v.t. administration were available to refine the PopPK model and, thus, more precisely predict the CSF concentration after i.v.t. administration of vancomycin. In this study, standard dosing recommendations for all populations are unrealistic due to the multitude of covariates, but dosing adjustment based on Bayesian prediction via the PopPK model might be a better option.

In this study, a PopPK model for vancomycin was successfully established using data from patients with EVD. Three substances quantified in CSF were identified as predictors associated with vancomycin CSF concentrations, and the relationship with CSF protein was the closest. The model fully supported the feasibility of collecting CSF samples at the distal port of the EVD system for TDM. Recommendations on dosing regimen for patients with CNS infection were provided according to different CSF protein levels. Beyond adjusting doses according to renal function, starting treatment with a loading dose in patients with primary CSF infection was recommended.

MATERIALS AND METHODS

Ethical approval. This study protocol was approved by the Institutional Review Board of the Medical Faculty of the Ludwig-Maximilians-Universität München (Munich, Germany) (approval number 20-169). The study is registered at ClinicalTrials.gov under registration no. NCT04426383. Written informed consent was obtained from all patients or their health care proxies.

Study design and data organization. This study was conducted at University Hospital of Munich, Germany. Adult patients who underwent EVD due to, e.g., ventriculitis, traumatic brain injury, or subarachnoid hemorrhage and who received vancomycin were recruited from August 2020 to September 2021. EVD systems remained open and, thus, provided continuous CSF draining. Patients were classified according to whether the primary infection was a CNS infection or not. Vancomycin was administered by intermittent infusion and/or continuous infusion (with or without an initial loading dose), as determined by the physician in charge. Blood samples and CSF samples from the proximal port (CSF_P) or distal port (CSF_D) of the EVD system were collected for measurements of vancomycin concentrations and clinical parameters (19). All samples were collected based on leftover materials from blood gas analyses, routine blood sampling, routine CSF sampling, and remaining CSF in the drainage reservoir.

The sample volumes and collecting times of CSF samples were documented, as well as basic demographic information, including age, sex, weight, and height. The actual time of the CSF_P samples is the respective recording time, while the actual time of the CSF_D samples was calculated with the following formula: (recording time) − (sampling duration)/2. The estimated drainage rate of CSF_D samples was then calculated with the formula (CSF_D sample volume)/(sample duration), and the estimated time delay (applied for the sensitivity analysis only) was then calculated with the formula (dead volume [7 mL])/(estimated drainage rate). The glomerular filtration rate (eGFR) was estimated using the Chronic Kidney Disease Epidemiology Collaboration (CKD-EPI) 2021 equation, creatinine clearance (CrCL) was estimated using the Cockcroft-Gault equation (39, 40), and body surface area (BSA) was calculated using the DuBois and DuBois equation (41).

Analytics. Vancomycin was quantified by high-performance liquid chromatography (HPLC)-UV spectroscopy using a Prominence LC20 modular HPLC system equipped with an SPD-M30A PDA detector (detection wavelength, 240 nm) and LabSolution software (Shimadzu, Duisburg, Germany). The autosampler was cooled to 6°C, and the column temperature was 40°C. Separation was performed using a

CORTECS T3 2.7-μm particle size, 100- by 3-mm column (Waters, Eschborn, Germany) preceded by a guard column (Nucleoshell RP 18, 2.7-μm particle size, 4 by 3 mm; Macherey-Nagel, Düren, Germany). The mobile phase consisted of 0.05 M sodium phosphate buffer with 7.86% (vol/vol) acetonitrile, pH adjusted to 3.6 or 2.9. At a flow rate of 0.4 mL/min, vancomycin eluted after 3.8 min at pH 3.6 or 5.1 min at pH 2.9. The total vancomycin concentrations in plasma were determined following a repeatedly described method for the analysis of beta-lactam antibiotics (42). The sample preparation included diluted phosphoric acid instead of phosphate buffer, to achieve quantitative recovery (43). In brief, plasma (100 μL) was acidified with 0.1 M *o*-phosphoric acid (200 μL) and mixed with acetonitrile (500 μL). After separation of the precipitated proteins and extraction of acetonitrile into dichloromethane (1.3 mL), an aliquot (2 μL) of the aqueous layer was injected into the HPLC system. Free vancomycin concentrations were determined after ultrafiltration as described previously (42). In brief, plasma (300 μL) was buffered with 10 μL of 3 M potassium phosphate (pH 7.4) in a Vivafree 500 30-kDa Hydrosart centrifugal ultrafiltration device (Vivaproducts, Inc., Littleton, MA, USA) and then incubated in a microcentrifuge (Eppendorf 5417R; Eppendorf, Hamburg, Germany) for 10 min at 100 $\times$ *g* and 37°C and centrifuged for 20 min at 1,000 $\times$ *g* and 37°C. An aliquot (0.5 μL) of the ultrafiltrate was injected into the HPLC system. CSF was centrifuged at 12,000 $\times$ *g* for 3 min, and an aliquot (0.5 μL) of the supernatant was injected into the HPLC system. Calibration was performed by external standardization, as no matrix effect is observed when using HPLC-UV, in contrast to liquid chromatography-tandem mass spectrometry (LC-MS/MS) (44). The linearity of the assay ($R > 0.998$) has been proven from 300 mg/L down to 0.3 mg/L in plasma and 0.1 mg/L in saline as a surrogate for CSF or ultrafiltrate, respectively. These lowest nonzero standards on the calibration curves were defined as the lower limit of quantification (LLOQ). Based on in-process quality controls (QCs; plasma of healthy subjects spiked with 80 mg/L, 25 mg/L, or 6.25 mg/L vancomycin) the coefficients of variation (CVs) of intra- and interassay determinations of total drug in plasma were <3% (imprecision), and the accuracy was 99.1%. The f_u of vancomycin in these QCs was 79.5% $\pm$ 1.6% (CV = 2.0%). The QCs were analyzed as single samples, as in preliminary experiments, the difference between duplicates was as low as 1%, i.e., in the range of the imprecision of the injection system. The accuracy regarding the determination of the free concentrations in plasma cannot be specified, as the extent of protein binding in a particular plasma sample is not known (45). The CVs of the intra- and interassay determinations of vancomycin in saline as a surrogate for CSF or ultrafiltrate (QCs of 5 mg/L and 0.5 mg/L) were <4% (imprecision), and the accuracy was 98.6%. The stability of the processed samples in the autosampler (16 to 18 h/6°C) was 98.3% $\pm$ 2.5% for total plasma concentrations, 99.4% $\pm$ 1.5% for free plasma concentrations, and 95.1% $\pm$ 7.2% for CSF concentrations.

Population pharmacokinetic modeling. The PopPK model was developed and diagnosed using the nonlinear mixed-effects model software NONMEM (version 7.4.0; ICON Development Solutions, USA) and Perl-speaks-NONMEM (PsN) (version 5.3.0; Uppsala University, Sweden) (46, 47). The model was developed using first-order conditional estimation with interaction, where a decrease of >3.84 in the objective function value (OFV) between 2 nested models ($P < 0.05$) upon the inclusion of a parameter was used as a statistical criterion. The nonnested models were compared using the Akaike information criterion (AIC), and the model with the lower AIC was selected (48). Covariates were assessed by stepwise forward inclusion ($P = 0.05$) using the stepwise covariate modeling tool in PsN. Statistics and graphic visuals were performed using R (version 4.2.0). The model was developed based on total vancomycin concentrations in plasma and CSF. Samples with concentrations below the limit of quantification (BLQ) were omitted during model development because the percentage of BLQ data was less than 2% (49).

The interindividual variables (IIVs) for PK parameters were described by the exponential equation $\theta_i = \theta \times e^{\eta_i}$, where θ_i is the value of the individual predicted parameter and θ is the population point estimate of the parameter. Different error models, including additive-only and proportional-only error models and the combination thereof, were evaluated separately. The plasma data were initially used to establish the basic model with one-, two-, and three-compartment model attempts. Subsequently, covariates related to plasma PK parameters were tested, including age, sex, weight, height, BSA, primary CNS infection, eGFR, and CrCL.

On the basis of the plasma model, a CSF compartment was directly linked to the central compartment with the intercompartment clearance between plasma and CSF (Q_{CSF}), as well as the CSF compartment volume (V_{CSF}). Two empirical methods to describe the elimination of the drug from the CSF compartment were tested separately. The first was to introduce a transit compartment between the CSF compartment and the central compartment with an independent parameter of transit compartment rate; in the meantime, the V_{CSF} was fixed to be weight $\times$ 0.002 L/kg based on the reported value of human CSF volume (Fig. 4, left) (50, 51). The other was to introduce an additional clearance, i.e., bulk flow (Q_{BULK} = 0.025 L/h), when the drug was eliminated from the CSF compartment to the central compartment (Fig. 4, right) (18, 52). The following covariates were assessed using the two models described above in parallel: age, sex, weight, height, BSA, primary CNS infection, drainage rate, CSF sample volume, unbound fraction (f_u), albumin, bilirubin, C-reactive protein, leukocytes, and interleukin 6 and neuron-specific enolase (CSF), S100 protein (CSF), ferritin (CSF), erythrocytes (CSF), cell count (CSF), protein (CSF), glucose (CSF), interleukin 6 (CSF), and lactate (CSF). After the development of a reasonable CSF base model using all CSF sample data, the role of the two types of CSF samples was investigated by comparison of parameter estimates when including and excluding the CSF_P samples and by separation of residual errors for CSF_P and CSF_D samples. Only forward inclusion was used for covariates based on significant improvement of the model, because of the small sample size and the exploratory type of evaluation. Exponential and proportional models were compared for continuous covariates, and conditional effects was used for categorical covariates.

Internal model evaluation of the final model was performed by individual plots of predicted concentrations and observed concentrations, goodness-of-fit (GOF) plots, and prediction-corrected visual predictive

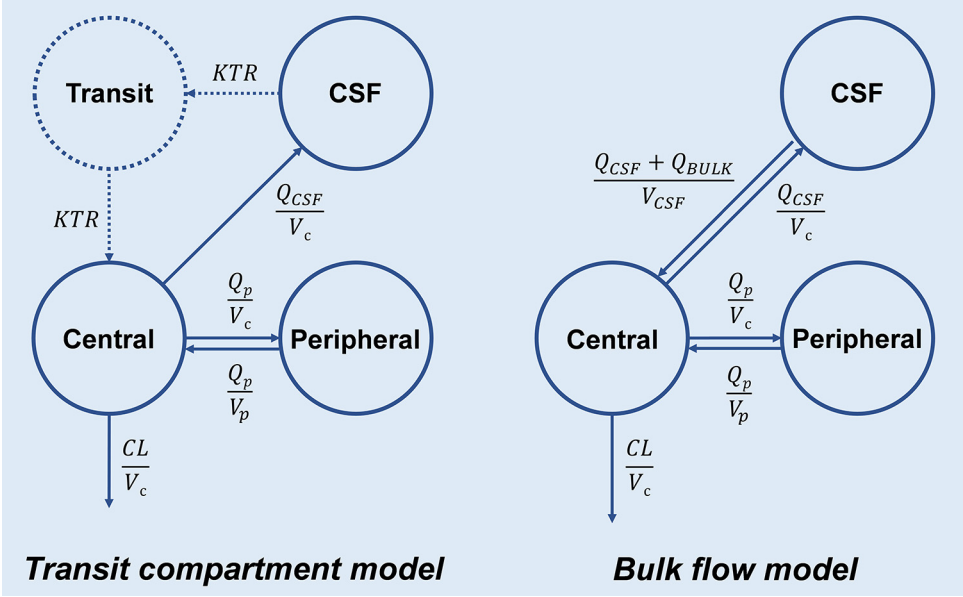

FIG 4 Scheme of the transit compartment model (left) and the bulk flow model (right; preferred and used for further evaluations) for the CSF compartment. In both models, vancomycin directly entered the central compartment with zero-order absorption. In the transit compartment model, vancomycin entered the CSF compartment from the central compartment (compartment volume, V_c) with an intercompartment clearance (Q_{CSF}), while the CSF compartment volume (V_{CSF}) was fixed at 0.002 L/kg × weight. Then, vancomycin returned to the central compartment through a separate transit compartment with an independent parameter transit rate (KTR). In the bulk flow model, vancomycin entered the CSF compartment from the central compartment with Q_{CSF}, but with an additional bulk flow (Q_{BULK}, 0.025 L/h) when vancomycin returned to the central compartment. Both models contain a peripheral compartment with the parameters intercompartment clearance (Q_p) and peripheral compartment volume (V_P). Vancomycin was ultimately eliminated by first order from the central compartment.

checks (pcVPC, n = 1,000) (53). Model stability and parameter precision were tested by a nonparametric bootstrap approach (n = 1,000 bootstraps).

To further assess a potential effect of the CSF sampling site on the results of the model, a sensitivity analysis was carried out. Although we were aware that the respective estimated time delay (calculated as described in "Study design and data organization," above) might not be reliable, to this end, CSF_D sampling times were adjusted by the individual estimated time delay with censoring of any adjusted times to the value of the previous shifted sampling time plus 0.01 h. Censoring was used to avoid disturbing the order of samples by this procedure. Parameter estimates and PTA calculation were compared between the final model and the model using data with adjusted times for CSF_D samples. We repeated this exercise with uniformly shifted CSF_D sampling times, assuming CSF flow rates of 12 and 36 mL/h, which reflects the reported range of CSF production rates (20).

Simulations. Different dosing regimens were tested separately in 3,000 simulated subjects with primary CNS infection on the basis of Monte Carlo simulations, where age, CrCL, and CSF protein concentrations were generated according to covariate distributions in our observational data. Three infusion modes, intermittent infusion, continuous infusion with a loading dose, and continuous infusion without a loading dose, were compared in terms of the daily area under the curve (AUC_{24}) in plasma and the trough concentration (C_{trough}; the concentration at 24 h or 120 h after the first dose for day 1 or steady state, respectively) in CSF, which are common PK/PD targets for vancomycin therapy (22, 33). For continuous infusion with a loading dose, the loading dose was chosen to be half of the daily dose on the first day of treatment, and the remaining daily dose was administered immediately after the loading dose was completed. From the second day, the daily dose was administered only by continuous infusion. Only total vancomycin concentrations in plasma and CSF were applied for PTA calculations, as a total vancomycin AUC/MIC of ≥400 has been advocated as a plasma target, while the protein binding of vancomycin in CSF is currently unknown and protein concentrations in CSF are negligible (3, 33).

SUPPLEMENTAL MATERIAL

Supplemental material is available online only.

SUPPLEMENTAL FILE 1, DOCX file, 0.7 MB.

ACKNOWLEDGMENTS

Zhendong Chen received a scholarship from the China Scholarship Council (CSC) for support of his Ph.D. studies. Chunli Chen was financed by the International Postdoctoral Exchange Fellowship Program from the Office of China Postdoctoral Council (grants

number 2020106 and PC2020013) and the National Natural Science Foundation of Heilongjiang Province (grant number YQ2022C017).

The funders had no role in design, collection, analysis and interpretation of data, and writing and publication of the manuscript.

REFERENCES

1. Beer R, Lackner P, Pfausler B, Schmutzhard E. 2008. Nosocomial ventriculitis and meningitis in neurocritical care patients. J Neurol 255:1617–1624. https://doi.org/10.1007/s00415-008-0059-8.
2. Blassmann U, Roehr AC, Frey OR, Vetter-Kerkhoff C, Thon N, Hope W, Briegel J, Huge V. 2016. Cerebrospinal fluid penetration of meropenem in neurocritical care patients with proven or suspected ventriculitis: a prospective observational study. Crit Care 20:343. https://doi.org/10.1186/s13054-016-1523-y.
3. Rybak M, Lomaestro B, Rotschafer JC, Moellering R, Jr, Craig W, Billeter M, Dalovisio JR, Levine DP. 2009. Therapeutic monitoring of vancomycin in adult patients: a consensus review of the American Society of Health-System Pharmacists, the Infectious Diseases Society of America, and the Society of Infectious Diseases Pharmacists. Am J Health Syst Pharm 66:82–98. https://doi.org/10.2146/ajhp080434.
4. Matzke GR, Zhanel GG, Guay DR. 1986. Clinical pharmacokinetics of vancomycin. Clin Pharmacokinet 11:257–282. https://doi.org/10.2165/00003088-198611040-00001.
5. Matzke GR, McGory RW, Halstenson CE, Keane WF. 1984. Pharmacokinetics of vancomycin in patients with various degrees of renal function. Antimicrob Agents Chemother 25:433–437. https://doi.org/10.1128/AAC.25.4.433.
6. Rodvold KA, Blum RA, Fischer JH, Zokufa HZ, Rotschafer JC, Crossley KB, Riff LJ. 1988. Vancomycin pharmacokinetics in patients with various degrees of renal function. Antimicrob Agents Chemother 32:848–852. https://doi.org/10.1128/AAC.32.6.848.
7. Ackerman BH, Taylor EH, Olsen KM, Abdel-Malak W, Pappas AA. 1988. Vancomycin serum protein binding determination by ultrafiltration. Drug Intell Clin Pharm 22:300–303. https://doi.org/10.1177/106002808802200404.
8. Golper TA, Noonan HM, Elzinga L, Gilbert D, Brummett R, Anderson JL, Bennett WM. 1988. Vancomycin pharmacokinetics, renal handling, and nonrenal clearances in normal human subjects. Clin Pharmacol Ther 43:565–570. https://doi.org/10.1038/clpt.1988.74.
9. Bailey EM, Rybak MJ, Kaatz GW. 1991. Comparative effect of protein binding on the killing activities of teicoplanin and vancomycin. Antimicrob Agents Chemother 35:1089–1092. https://doi.org/10.1128/AAC.35.6.1089.
10. Monteiro JF, Hahn SR, Gonçalves J, Fresco P. 2018. Vancomycin therapeutic drug monitoring and population pharmacokinetic models in special patient subpopulations. Pharmacol Res Perspect 6:e00420. https://doi.org/10.1002/prp2.420.
11. Broeker A, Nardecchia M, Klinker KP, Derendorf H, Day RO, Marriott DJ, Carland JE, Stocker SL, Wicha SG. 2019. Towards precision dosing of vancomycin: a systematic evaluation of pharmacometric models for Bayesian forecasting. Clin Microbiol Infect 25:1286.e1–1286.e7. https://doi.org/10.1016/j.cmi.2019.02.029.
12. Lutsar I, McCracken GH, Jr, Friedland IR. 1998. Antibiotic pharmacodynamics in cerebrospinal fluid. Clin Infect Dis 27:1117–1127. https://doi.org/10.1086/515003.
13. Rybak MJ. 2006. The pharmacokinetic and pharmacodynamic properties of vancomycin. Clin Infect Dis 42(Suppl 1):S35–S39. https://doi.org/10.1086/491712.
14. Popa D, Loewenstein L, Lam SW, Neuner EA, Ahrens CL, Bhimraj A. 2016. Therapeutic drug monitoring of cerebrospinal fluid vancomycin concentration during intraventricular administration. J Hosp Infect 92:199–202. https://doi.org/10.1016/j.jhin.2015.10.017.
15. Beach JE, Perrott J, Turgeon RD, Ensom MHH. 2017. Penetration of vancomycin into the cerebrospinal fluid: a systematic review. Clin Pharmacokinet 56:1479–1490. https://doi.org/10.1007/s40262-017-0548-y.
16. Li X, Wu Y, Sun S, Mei S, Wang J, Wang Q, Zhao Z. 2015. Population pharmacokinetics of vancomycin in postoperative neurosurgical patients. J Pharm Sci 104:3960–3967. https://doi.org/10.1002/jps.24604.
17. Li X, Wu Y, Sun S, Zhao Z, Wang Q. 2016. Population pharmacokinetics of vancomycin in postoperative neurosurgical patients and the application in dosing recommendation. J Pharm Sci 105:3425–3431. https://doi.org/10.1016/j.xphs.2016.08.012.
18. Jalusic KO, Hempel G, Arnemann PH, Spiekermann C, Kampmeier TG, Ertmer C, Gastine S, Hessler M. 2021. Population pharmacokinetics of vancomycin in patients with external ventricular drain-associated ventriculitis. Br J Clin Pharmacol 87:2502–2510. https://doi.org/10.1111/bcp.14657.
19. Kinast CB, Paal M, Liebchen U. 2022. Comparison of cerebrospinal fluid collection through the proximal and distal port below the overflow system from an external ventricular drain. Neurocrit Care 37:775–778. https://doi.org/10.1007/s12028-022-01615-y.
20. Beidler PG, Novokhodko A, Prolo LM, Browd S, Lutz BR. 2021. Fluidic considerations of measuring intracranial pressure using an open external ventricular drain. Cureus 13:e15324. https://doi.org/10.7759/cureus.15324.
21. Sinha Ray A, Haikal A, Hammoud KA, Yu AS. 2016. Vancomycin and the risk of AKI: a systematic review and meta-analysis. Clin J Am Soc Nephrol 11:2132–2140. https://doi.org/10.2215/CJN.05920616.
22. Rybak MJ, Le J, Lodise TP, Levine DP, Bradley JS, Liu C, Mueller BA, Pai MP, Wong-Beringer A, Rotschafer JC, Rodvold KA, Maples HD, Lomaestro BM. 2020. Therapeutic monitoring of vancomycin for serious methicillin-resistant Staphylococcus aureus infection: a revised consensus guideline and review by the American Society of Health-System Pharmacists, the Infectious Diseases Society of America, the Pediatric Infectious Diseases Society, and the Society of Infectious Diseases Pharmacists. Am J Health Syst Pharm 77:835–864. https://doi.org/10.1093/ajhp/zxaa036.
23. Yamamoto M, Kuzuya T, Baba H, Yamada K, Nabeshima T. 2009. Population pharmacokinetic analysis of vancomycin in patients with gram-positive infection and the influence of infectious disease type. J Clin Pharm Ther 34:473–483. https://doi.org/10.1111/j.1365-2710.2008.01016.x.
24. Deng C, Liu T, Zhou T, Lu H, Cheng D, Zhong X, Lu W. 2013. Initial dosage regimens of vancomycin for Chinese adult patients based on population pharmacokinetic analysis. Int J Clin Pharmacol Ther 51:407–415. https://doi.org/10.5414/CP201842.
25. Ishikawa M, Yamazaki S, Suzuki T, Uchida M, Iwadate Y, Ishii I. 2019. Correlation between vancomycin penetration into cerebrospinal fluid and protein concentration in cerebrospinal fluid/serum albumin ratio. J Infect Chemother 25:124–128. https://doi.org/10.1016/j.jiac.2018.10.013.
26. Chow E, Troy SB. 2014. The differential diagnosis of hypoglycorrhachia in adult patients. Am J Med Sci 348:186–190. https://doi.org/10.1097/MAJ.0000000000000217.
27. Pleines UE, Morganti-Kossmann MC, Rancan M, Joller H, Trentz O, Kossmann T. 2001. S-100 beta reflects the extent of injury and outcome, whereas neuronal specific enolase is a better indicator of neuroinflammation in patients with severe traumatic brain injury. J Neurotrauma 18:491–498. https://doi.org/10.1089/089771501300227297.
28. Wang J, Chen S, Wang X, Gu H, Liu J, Wang X, Liu L. 2019. Value of NSE and S100 protein of Kawasaki disease with aseptic meningitis in infant. Open Life Sci 14:358–362. https://doi.org/10.1515/biol-2019-0040.
29. Wong FW. 2011. Cerebrospinal fluid collection: a comparison of different collection sites on the external ventricular drain. Dynamics 22:19–24.
30. Alihodzic D, Broeker A, Baehr M, Kluge S, Langebrake C, Wicha SG. 2020. Impact of inaccurate documentation of sampling and infusion time in model-informed precision dosing. Front Pharmacol 11:172. https://doi.org/10.3389/fphar.2020.00172.
31. Giuliano C, Haase KK, Hall R. 2010. Use of vancomycin pharmacokinetic-pharmacodynamic properties in the treatment of MRSA infection. Expert Rev Anti Infect Ther 8:95–106. https://doi.org/10.1586/eri.09.123.
32. Aljefri DM, Avedissian SN, Rhodes NJ, Postelnick MJ, Nguyen K, Scheetz MH. 2019. Vancomycin area under the curve and acute kidney injury: a meta-analysis. Clin Infect Dis 69:1881–1887. https://doi.org/10.1093/cid/ciz051.
33. Blassmann U, Hope W, Roehr AC, Frey OR, Vetter-Kerkhoff C, Thon N, Briegel J, Huge V. 2019. CSF penetration of vancomycin in critical care patients with proven or suspected ventriculitis: a prospective observational study. J Antimicrob Chemother 74:991–996. https://doi.org/10.1093/jac/dky543.
34. Hanrahan TP, Harlow G, Hutchinson J, Dulhunty JM, Lipman J, Whitehouse T, Roberts JA. 2014. Vancomycin-associated nephrotoxicity in the critically

ill: a retrospective multivariate regression analysis. Crit Care Med 42:2527–2536. https://doi.org/10.1097/CCM.0000000000000514.
35. Jankovska E, Svitek M, Holada K, Petrak J. 2019. Affinity depletion versus relative protein enrichment: a side-by-side comparison of two major strategies for increasing human cerebrospinal fluid proteome coverage. Clin Proteom 16:9. https://doi.org/10.1186/s12014-019-9229-1.
36. Ng K, Mabasa VH, Chow I, Ensom MH. 2014. Systematic review of efficacy, pharmacokinetics, and administration of intraventricular vancomycin in adults. Neurocrit Care 20:158–171. https://doi.org/10.1007/s12028-012-9784-z.
37. Chen K, Wu Y, Wang Q, Wang J, Li X, Zhao Z, Zhou J. 2015. The methodology and pharmacokinetics study of intraventricular administration of vancomycin in patients with intracranial infection after craniotomy. J Crit Care 30:218.e1–218.e5. https://doi.org/10.1016/j.jcrc.2014.09.020.
38. Li X, Sun S, Ling X, Chen K, Wang Q, Zhao Z. 2017. Plasma and cerebrospinal fluid population pharmacokinetics of vancomycin in postoperative neurosurgical patients after combined intravenous and intraventricular administration. Eur J Clin Pharmacol 73:1599–1607. https://doi.org/10.1007/s00228-017-2313-4.
39. Meeusen JW, Kasozi RN, Larson TS, Lieske JC. 2022. Clinical impact of the refit CKD-EPI 2021 creatinine-based eGFR equation. Clin Chem 68:534–539. https://doi.org/10.1093/clinchem/hvab282.
40. Cockcroft DW, Gault MH. 1976. Prediction of creatinine clearance from serum creatinine. Nephron 16:31–41. https://doi.org/10.1159/000180580.
41. DuBois D, DuBois EF. 1916. A formula to estimate the approximate surface area if height and weight be known. Arch Intern Med 17:863.
42. Dorn C, Kratzer A, Schießer S, Kees F, Wrigge H, Simon P. 2019. Determination of total or free cefazolin and metronidazole in human plasma or interstitial fluid by HPLC-UV for pharmacokinetic studies in man. J Chromatogr B Analyt Technol Biomed Life Sci 1118–1119:51–54. https://doi.org/10.1016/j.jchromb.2019.04.025.
43. Beckmann J, Kees F, Schaumburger J, Kalteis T, Lehn N, Grifka J, Lerch K. 2007. Tissue concentrations of vancomycin and moxifloxacin in periprosthetic infection in rats. Acta Orthop 78:766–773. https://doi.org/10.1080/17453670710014536.
44. An G, Bach T, Abdallah I, Nalbant D. 2020. Aspects of matrix and analyte effects in clinical pharmacokinetic sample analyses using LC-ESI/MS/MS—two case examples. J Pharm Biomed Anal 183:113135. https://doi.org/10.1016/j.jpba.2020.113135.
45. Nilsson LB. 2013. The bioanalytical challenge of determining unbound concentration and protein binding for drugs. Bioanalysis 5:3033–3050. https://doi.org/10.4155/bio.13.274.
46. Boeckmann A, Sheiner L, Beal S. 2001. NONMEM users guide—part V. University of California, San Francisco, CA.
47. Lindbom L, Pihlgren P, Jonsson EN. 2005. PsN-Toolkit—a collection of computer intensive statistical methods for non-linear mixed effect modeling using NONMEM. Comput Methods Programs Biomed 79:241–257. https://doi.org/10.1016/j.cmpb.2005.04.005.
48. Mould DR, Upton RN. 2013. Basic concepts in population modeling, simulation, and model-based drug development—part 2: introduction to pharmacokinetic modeling methods. CPT Pharmacometrics Syst Pharmacol 2:e38. https://doi.org/10.1038/psp.2013.14.
49. Irby DJ, Ibrahim ME, Dauki AM, Badawi MA, Illamola SM, Chen M, Wang Y, Liu X, Phelps MA, Mould DR. 2021. Approaches to handling missing or "problematic" pharmacology data: pharmacokinetics. CPT Pharmacometrics Syst Pharmacol 10:291–308. https://doi.org/10.1002/psp4.12611.
50. Büsker S, Jäger W, Poschner S, Mayr L, Al Jalali V, Gojo J, Azizi AA, Ullah S, Bilal M, El Tabei L, Fuhr U, Peyrl A. 2022. Pharmacokinetics of metronomic temozolomide in cerebrospinal fluid of children with malignant central nervous system tumors. Cancer Chemother Pharmacol 89:617–627. https://doi.org/10.1007/s00280-022-04424-4.
51. Miller RD. 2020. Miller's anesthesia, 9th ed. Elsevier, Philadelphia, PA.
52. Segal MB. 1993. Extracellular and cerebrospinal fluids. J Inherit Metab Dis 16:617–638. https://doi.org/10.1007/BF00711896.
53. Bergstrand M, Hooker AC, Wallin JE, Karlsson MO. 2011. Prediction-corrected visual predictive checks for diagnosing nonlinear mixed-effects models. AAPS J 13:143–151. https://doi.org/10.1208/s12248-011-9255-z.